Mon. Not. R. Astron. Soc. **000**, 000–000 (0000) Printed 30 July 1997 (MN LATEX style file v1.4)

The changing face of Betelgeuse

R.W. Wilson[1], V.S. Dhillon[1], and C.A. Haniff[2]
[1] *Royal Greenwich Observatory, Madingley Road, Cambridge, UK CB3 0EZ*
[2] *Mullard Radio Astronomy Observatory, Cavendish Laboratory, Madingley Road, Cambridge, UK CB3 0HE*

30 July 1997

ABSTRACT
We describe a sequence of four optical interferometric observations of Betelgeuse, obtained using the non-redundant aperture mask method at the 4.2-m William Herschel Telescope on La Palma between 1994 November and 1995 January. The observations reveal complex asymmetries in the brightness distribution of the star, detected at a very high signal-to-noise ratio. Adequate modelling of the intensity structure requires at least three bright spots superposed on the stellar disk. Changes in the relative flux and positions of the spots are evident over the eight week period spanning the observations. The brightness and maximum size of these features are consistent with convective surface hot-spots. Simultaneous photometry of the integrated light of Betelgeuse shows a large and rapid dimming over the same period, which is not correlated with any change in the bright features. We deduce that, in this instance, the photometric variation did not result from localised convective activity associated with the spots. The interferometric data also show strong evidence for structure on a scale much larger than the photospheric diameter, which has not been present in previous observations over recent years. We attribute this new component to scattering from a newly formed dust halo, with a minimum angular diameter of approximately $0.3''$. Since the brightness of this structure relative to the stellar disk did not change significantly throughout our observations, it is unlikely that the dimming of the star resulted from increased absorption by the dust halo. We conclude that the fading was due to a global expansion and cooling of the photosphere.

Key words: stars: individual: Betelgeuse – stars: circumstellar matter – stars: late type – stars: mass loss – stars: variable: other – techniques: interferometric.

1 INTRODUCTION

In recent years, diffraction-limited optical aperture synthesis observations have consistently revealed bright, asymmetric features in the intensity distribution of the red supergiant star Betelgeuse. Maps made by the Cambridge group using the non-redundant mask (NRM) method, have in all cases shown strong asymmetries, which have been well modelled as unresolved bright features superposed on the stellar disk (Buscher et al. 1990; Wilson et al. 1992; Tuthill, Haniff & Baldwin 1997). However, the position, brightness, and number of features detected in these NRM observations have been different at each epoch. Since the shortest interval between observations before 1994 has been four months, the timescale for changes on the surface is assumed to be $\sim$100 days or less. The favoured physical explanation for the bright features is that they are surface hot-spots resulting from large scale photospheric turbulence. The observed changes are assumed to result from the growth and decay of individual features, with continual convective 'boiling' at the surface.

Such transient convective features have often been implicated to explain the irregular photometric and polarimetric fluctuations of Betelgeuse which occur on timescales of a few weeks to months (Tinbergen, Greenberg & de Jager 1981; Hayes 1981; Antia et al. 1984; Goldberg 1984; Schwarz 1984). However this hypothesis has never been examined directly via contemporaneous high resolution imaging and photometric or polarimetric monitoring.

In this paper we present a sequence of four NRM observations of Betelgeuse made between 1994 November and 1995 January in order to monitor changes in the stellar brightness distribution over short timescales. We also report contemporaneous V-band photometric measurements from the Carlsberg Automated Meridian Circle (CAMC) on La Palma. These combined data have allowed us to investigate for the first time whether variations in the integrated magnitude can be related directly to changes in the surface morphology of the star.

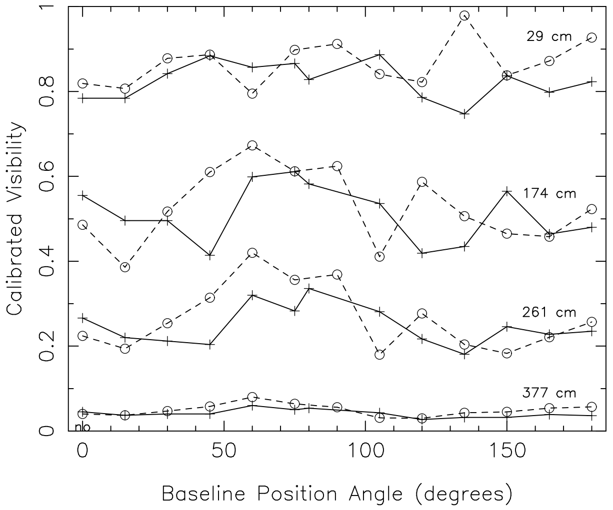

Figure 1. Calibrated visibilities for Betelgeuse as measured on 1994 December 24. Visibilities are plotted for four baseline lengths: 31 cm, 174 cm, 261 cm, and 377 cm. Each plotted point is the averaged value for 3000 interferograms. The solid and dashed lines show the amplitudes for two independently calibrated data sets, recorded on the same night with an interval of approximately two hours. Differences between the two data sets indicate the magnitude of the systematic errors associated with calibration.

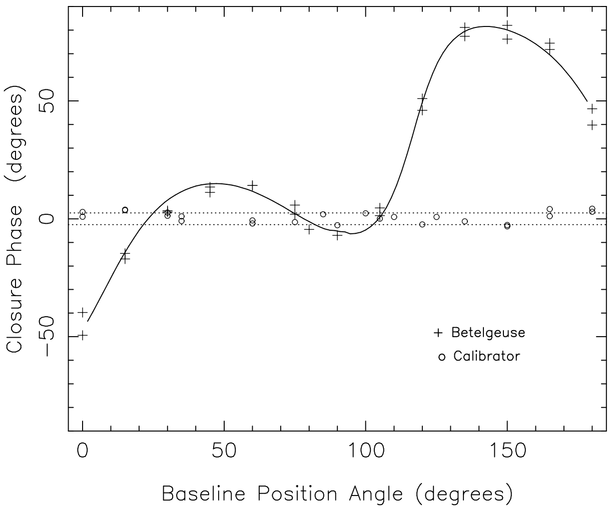

Figure 2. Closure phases for Betelgeuse measured on 1994 December 24. Each plotted point is the averaged value from 3000 interferograms. For most position angles, two points are plotted. These represent results from two independent data sets, recorded on the same night at an interval of approximately two hours. The rms difference between the two data sets indicates the uncertainty due to residual atmospheric noise, and is $\simeq 2.5°$ in this case. The dotted lines delimit this range of uncertainty relative to the origin. Note that the values for the calibrator are zero to within the typical error, so that the closure phases for Betelgeuse require no calibration. The solid line is the closure phase for the best-fit 5 component model at this epoch (see section 3).

2 OBSERVATIONS AND DATA REDUCTION

NRM observations were made using the GHRIL facility at the Nasmyth focus of the William Herschel Telescope (WHT) on La Palma. Data of good signal-to-noise ratio were obtained on the following four nights: 1994 November 24, 1994 December 9, 1994 December 24, and 1995 January 17.

NRM is a well established technique which allows diffraction-limited mapping of bright, compact astronomical objects at visible wavelengths. The experimental procedure for NRM has been described in detail elsewhere (Haniff et al. 1987; Wilson et al. 1992; Bedding, Robertson & Marson 1994), and is only summarised briefly here. The method is similar to speckle interferometry, in that diffraction-limited object information is recovered from a Fourier analysis of a large number of short exposure images. In NRM, an aperture mask is used to isolate a number of small sub-apertures in the telescope pupil. This greatly reduces the effects of seeing on the measurements. The analysis also incorporates elements of aperture synthesis mapping, in that object Fourier phase information (which is corrupted by the effects of seeing) is recovered via the closure phase (Pearson & Readhead 1984).

For the experiments reported here, the optical configuration was essentially that of a Fizeau interferometer. The telescope pupil was imaged onto an aperture mask, which was opaque except for an array of five sub-apertures in a non-redundant configuration (i.e. with each sub-aperture separation occurring only once). Starlight emerging from the mask was focussed to form a fringe pattern on a CCD detector. As in previous observations, a co-linear array of sub-apertures was employed to allow fast-framing of the CCD through on-chip compression of the fringe pattern. The sub-apertures had an effective diameter of 16 cm when projected onto the telescope primary mirror, and defined a set of ten interferometer baselines, with a maximum length of 3.77 m. With this optical arrangement, the telescope measures the spatial coherence function of the object (i.e. the Fourier transform of the intensity distribution) at ten spatial frequencies corresponding to the ten baselines. Two dimensional sampling of the coherence function was achieved by changing the orientation of the interferometer with respect to the sky, using the telescope image rotator. The CCD camera was framed at 35 Hz, so that atmospheric distortions were effectively "frozen" in each 29-ms exposure. An optical bandpass of 10 nm centred at 700 nm was used. This wavelength was chosen as a compromise between spatial resolution (linear with wavelength), and noise on the visibility measurements introduced by the effects of seeing (a very strong inverse function of wavelength). The narrow bandpass was required to achieve high fringe contrast for baselines of up to 4 m.

Visibility amplitudes were estimated from the averaged image power spectrum for typically 3000 short exposure CCD images. The amplitudes were calibrated for seeing and other effects using measurements of unresolved stars observed at close to the same elevation. The calibration stars used were Procyon and Rigel. We chose the brightest calibration stars available, in order to minimise photon and detector read-out noise effects in the data. Note that for some epochs, independent calibrations were made using both calibration stars. In these cases we found no systematic differences between the two data-sets, and the results were the same to within the estimated uncertainties. In practice, though, the seeing often changed significantly between observations of source and calibrator separated in time by only a few minutes, thus limiting the accuracy of amplitude calibration. Figure 1 shows the calibrated visibility amplitude as a function of sky position angle, for four different baseline lengths measured on 1994 December 24. Two independently calibrated sets of measurements are plotted, for data recorded on the same night at an interval of approximately two hours. The discrepancy between the two data sets provides an estimate of the visibility amplitude calibration errors, which were typically 5–10% of the measured visibility. The observing conditions at each epoch varied somewhat: the data from December 24 were obtained in excellent seeing ($\approx 0.5''$ image FWHM), those from December 9 and January 17 in moderate seeing ($\approx 1.0''$), and those from November 24 in poorer conditions ($\approx 1.5''$).

Fourier phase retrieval was performed using bispectrum techniques. Although the visibility phases in each interferogram were corrupted by random phases introduced by atmospheric seeing, "uncontaminated" object phase information could be recovered using the closure phase, i.e. the sum of the fringe phases around a closed triangle of three interferometer baselines. The closure phase was derived from the data as the argument of the mean image bi-spectrum (Haniff et al. 1987).

Figure 2 shows examples of the closure phases measured on a single triangle of baselines for Betelgeuse and its calibrator Procyon, on 1994 December 24. Two independent data sets are plotted to give an indication of the errors on the closure phases. These were typically $\pm 2.5^\circ$. In this and all other cases, the closure phase values for the calibration star were zero to within the estimated uncertainties at all position angles, indicating that they were unbiased by atmospheric or optical distortions. The closure phases for Betelgeuse therefore required no calibration.

The final step of the data analysis procedure was to infer the source intensity distribution by fitting models to the measured visibility amplitude and closure phase data. Since the plots of visibility amplitude and closure phase were simple functions, varying only slowly with position angle, good fits could be obtained using models with a small number (< 15) of free parameters. The image plane scale and orientation of our optical set-up were calibrated using NRM observations of the binary star ϵ Hya, recorded at each observing epoch.

3 RESULTS

Figure 3 shows the azimuthally averaged calibrated visibilities for Betelgeuse as a function of baseline length for each observation. For long baselines (> 2 m) the visibilities are similar to those measured in previous NRM observations at this wavelength, for which the first minimum of the visibility function was at baseline lengths close to 4.0 m. At the longest baseline (3.77 m) the visibility has fallen smoothly to a value of approximately 0.04.

However, an important and unexpected result is that, for the observations reported here, the value of the calibrated visibility for the shortest baseline (29 cm) was significantly less than 1.0. In our previous NRM observations of Betelgeuse, the azimuthally averaged visibility on baselines of this, or similar, length have been close to unity. Here we find visibilities close to 0.83 ± 0.02 for each epoch.

One possible cause for low calibrated visibilities is a seeing mismatch between observations of the source and calibration stars. This might occur, for example, if the source were observed at a lower elevation than the calibrator. For the observations reported here, there were sometimes elevation differences of up to 10 degrees. However, both positive and negative elevation differences occurred, and the mean difference was always close to zero for each sequence of observations. In fact, the calibrated visibility showed no correlation with source/calibrator elevation difference. It is also unlikely that scattered light within our instrument could have produced such an effect in the calibrated visibilities, since observations of the source and calibrator would have been affected identically.

These latest observations thus provide unambiguous evidence for the appearance of a new large scale component in the brightness distribution of Betelgeuse. The new feature is resolved on a baseline of only 0.29 m, and is therefore much larger than the stellar disk. In the model fitting procedure, a good fit to the visibilities on the shortest baselines could be obtained by including a circular component with a Gaussian radial intensity profile, and a FWHM $\gtrsim 300$ milli-arcseconds (mas), contributing approximately 17% of the total model flux. The effect of neglecting this larger scale component in the model fitting is shown in the lowest panel of Figure 3: at short baselines the agreement between a model excluding a large scale halo and the data is clearly unacceptable. Since this large scale structure was completely resolved on even the shortest baseline, its radial profile was not well constrained. Good fits could also be obtained using a uniform circular disk (diameter $\gtrsim 400$ mas), or an optically thin spheroid ($\gtrsim 400$ mas).

As shown in Figure 2 the closure phases for Betelgeuse were large, and changed systematically with sky position angle. Non-zero closure phases are indicative of asymmetric structure and so modelling of the Fourier data was performed using both symmetric and asymmetric components. At each epoch, the simplest model for which a good fit to the data could be obtained consisted of:

(i) a uniform circular disk, which we assume corresponds to the photosphere of the star;
(ii) a larger (concentric) Gaussian component, required to fit the short baseline visibilities, as discussed above;
(iii) three superposed bright "spots", required to give a satisfactory fit to the closure phase data (see below). For simplicity these were modelled as circularly symmetric Gaussians.

It is important to note that for a model consisting of only the uniform circular disk and larger scale Gaussian component, the closure phases at all position angles are zero, since the model is circularly symmetric. If we take this featureless symmetric model as the "null hypothesis", it is re-

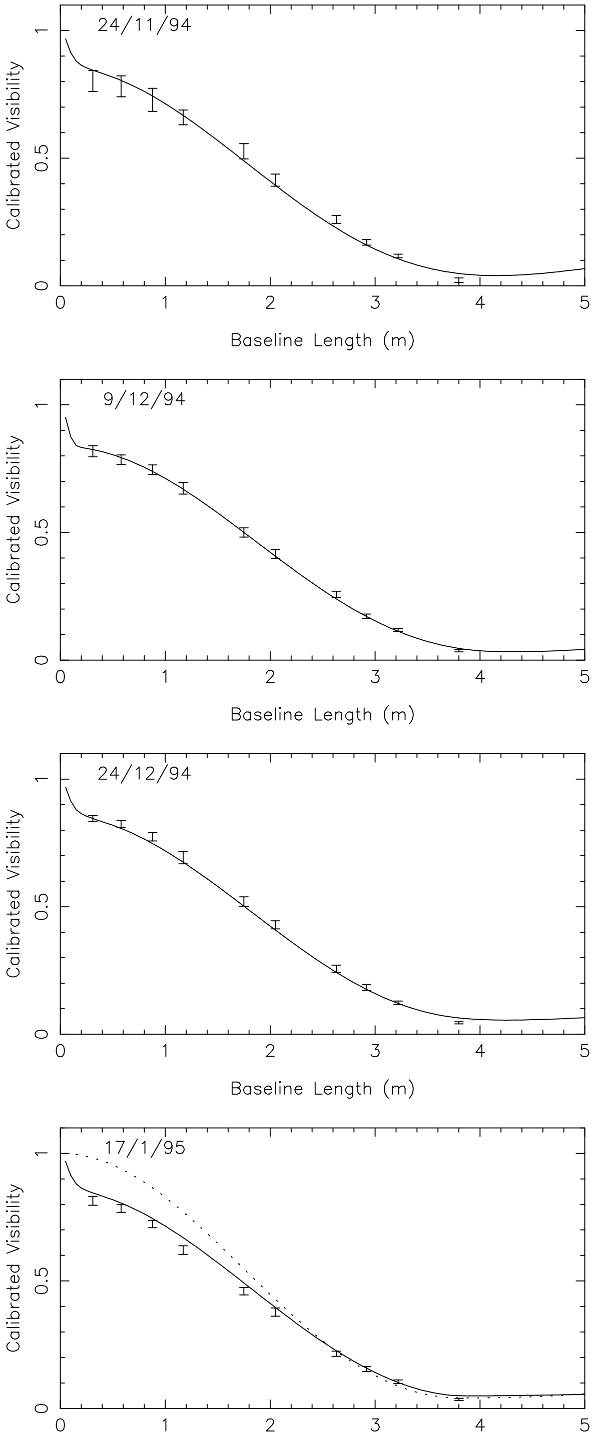

Figure 3. Azimuthally averaged visibilities for Betelgeuse at the four observing epochs. Solid lines are the azimuthally averaged visibilities for the best-fit 5 component (3 spot) model in each case (see text). For the data from January 17 we have also plotted the best-fit visibilities for a model in which the large scale structure is omitted (dotted line). This gives a very poor fit to the data.

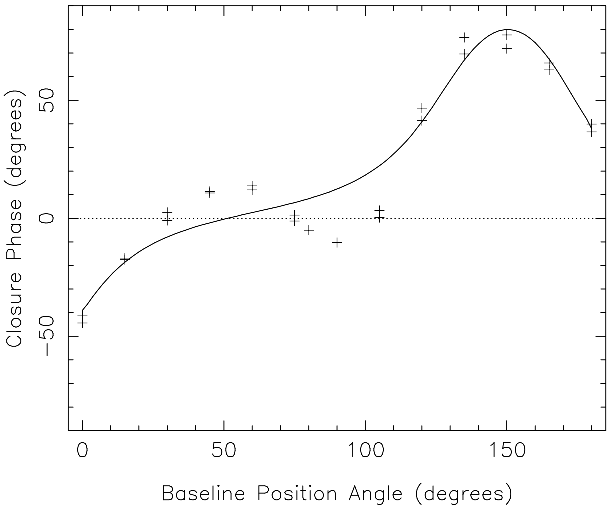

Figure 4. Measured closure phases for Betelgeuse on 24/12/94, and (solid line) closure phases for the best-fit 4 component (disk, halo and 2 spots) model (see text). This demonstrates the poor fit to the data obtained in this case.

jected with a probability > 0.9999 (reduced $\chi^2 \approx 20$). Models containing only one or two superposed spots also gave poor fits to the closure phase data (for example, see Figure 4). The surface asymmetry was therefore a relatively complex structure, requiring at least three additional components to give a satisfactory model fit.

Figure 5 shows the closure phases for Betelgeuse on one triangle of baselines, as a function of interferometer position angle, for each of the four observations. Also plotted are the closure phases for the best-fit model at each epoch. Simultaneous fits to all of the measured closure phases allowed the azimuthal positions of the superposed spots to be constrained to approximately 5°. The FWHM of the superposed bright features were limited to $\lesssim 15$ mas, since larger spot sizes did not allow excursions in the closure phases as large as were measured. Their minimum size, however, could not be determined precisely, and adequate fits could be obtained using components with sizes in the range 0–15 mas.

Between 1994 November 24 and December 24 the variation of closure phase with interferometer position angle displayed only a limited evolution, and changes in the locations of the model components were correspondingly small. Over this period the peak amplitude of the closure phase signal showed a gradual increase from $\approx 60^\circ$on 1994 November 24 to $\approx 80^\circ$on 1994 December 24. This change could be well modelled by a slight relative brightening of the superposed spots. However, by 1995 January 17 the behaviour of the closure phases had changed significantly, showing a discontinuity at position angle $\sim 15^\circ$. At this epoch the source was slightly more resolved along this direction, so that the visibility amplitude on the longest baseline was reduced to zero. This resulted in the discontinuity for closure phases involving this baseline. A five component (3 spot) model was again required to obtain a satisfactory fit, although in this case the azimuthal positions of the spots had changed from their values three weeks earlier.

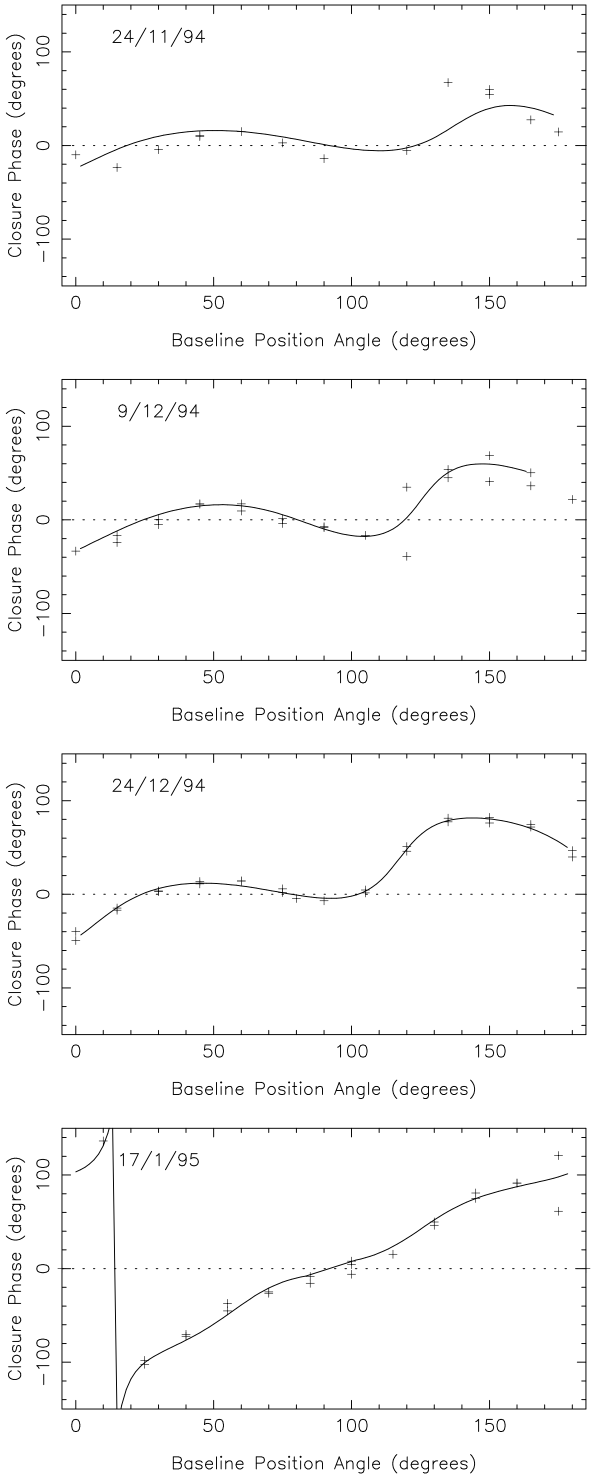

Figure 5. Measured closure phases for Betelgeuse at the four observing epochs. Solid lines are the closure phases for the best-fit 5 component (disk, halo and 3 spots) model in each case (see text). Note the discontinuity which appears in the closure phase function for 1995 January 17.

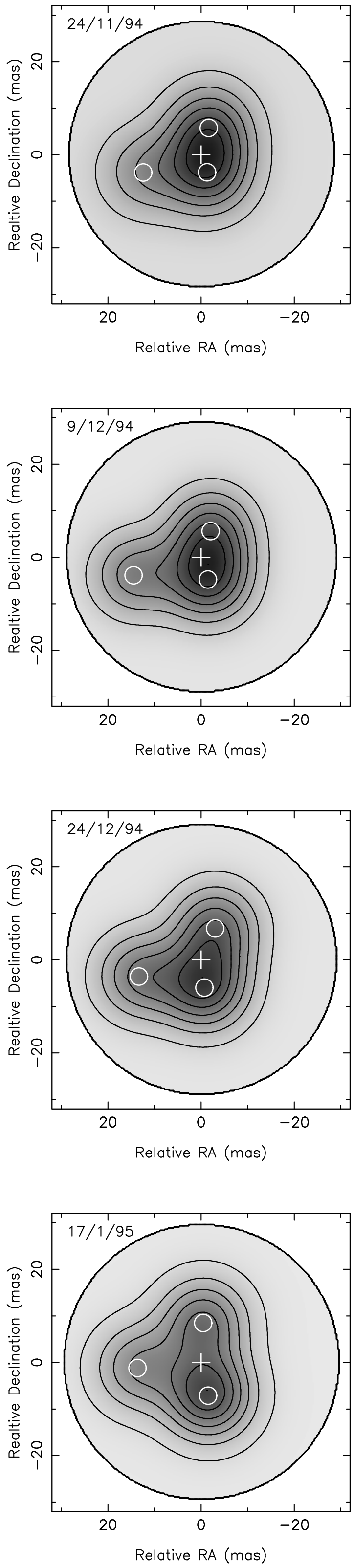

Figure 6. Grey scale and contour representations of the best-fit (3 spot) models for Betelgeuse (see table 1). Note that brighter areas are shaded *darker*. Contours are at 30,...90% of the peak flux (lower level contours are superposed at the edge of the disk). Small circles locate the centers of the spot components on the models, and the map center is marked with a plus sign. For clarity, the large scale Gaussian halo component is omitted from these maps. North is to the top and East to the left.

Table 1. Model data for Betelgeuse. For each epoch, the model is composed of a uniform circular disk, a concentric circular Gaussian 'halo' component with FWHM = 600 mas, plus three superposed Gaussian spots with FWHM = 12.5 mas. The table gives the fraction of the total flux contributed by each component. The halo flux contribution is fixed at 0.17. For the spots, D is their radial distance from the map centre in milli-arcseconds, and θ is their position angle in degrees measured North through East. For the disk component, D is the best-fit diameter (mas). Our data only constrain the FWHM of the large scale component to lie in the range 300–1000 mas: the values of the other model parameters are independent of this diameter. The uncertainties quoted are the one sigma confidence limits for each parameter assuming that all other parameters are held constant.

Component	Fractional flux ±0.020	D (mas) ±2 mas	θ (degrees) $\pm5°$
24/11/94			
Halo	0.170	-	-
Disk	0.625	56.8	-
Spot	0.046	13.1	107
Spot	0.086	4.0	199
Spot	0.074	6.1	344
9/12/94			
Halo	0.170	-	-
Disk	0.596	58.3	-
Spot	0.062	15.0	105
Spot	0.097	4.6	197
Spot	0.075	6.1	340
24/12/94			
Halo	0.170	-	-
Disk	0.592	57.5	-
Spot	0.066	13.8	105
Spot	0.097	5.9	187
Spot	0.076	7.4	336
17/1/95			
Halo	0.170	-	-
Disk	0.602	59.2	-
Spot	0.056	13.7	95
Spot	0.098	7.3	192
Spot	0.074	8.5	357

A summary of the best-fit model parameters is given in Table 1, and the models themselves are displayed as contour plots in figure 6. We have also inverted the data via a radio astronomy VLBI program which uses the maximum entropy method (Sivia 1989). The resulting maps are consistent with the model reconstructions shown in figure 6.

Some discussion of the uniqueness of these model fits is appropriate. The parameters given are for the best (least-squares) fit solution found by model fitting. However, other models were possible within the estimated uncertainties. In particular, the radial distribution of the flux in the models was less well constrained than its azimuthal distribution. For example, adequate fits to the data could be obtained by moving the spot components radially outward in the map by up to 5 mas (without changing their azimuthal position), while reducing their flux contribution. This ambiguity results from the relatively large uncertainties on the visibility amplitudes, due mainly to calibration errors as described in section 2. In contrast, the azimuthal positions were well constrained (to within $\pm5°$) by the closure phase measurements, which had much smaller uncertainties.

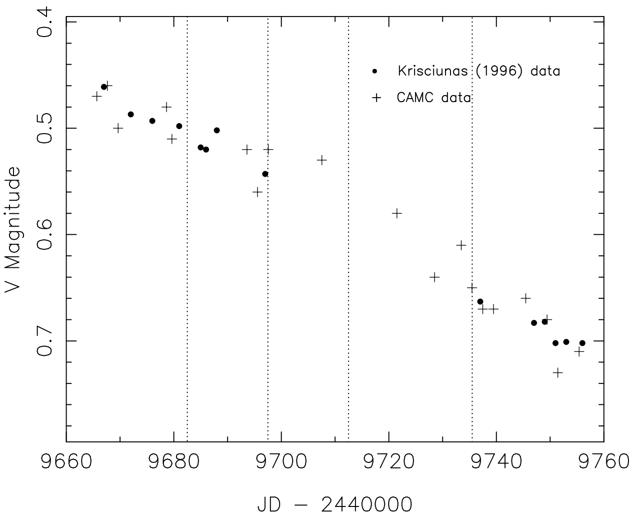

Figure 7. CAMC V-band photometric data for October 1994 to February 1995, showing the rapid dimming of Betelgeuse over this period. Also shown are the data of Krisciunas & Luedeke (1996). The vertical dotted lines indicate the epochs of the four WHT interferometric observations.

In order to correlate any observed surface changes with photometric variations of Betelgeuse, V-band magnitudes were obtained at the CAMC from 1994 November to 1995 February. These are plotted in figure 7, along with the data of Krisciunas & Luedeke (1996) for the same period. These show an increase of approximately 0.15 magnitudes from V=0.51 on 1994 November 24 to V=0.66 on 1995 January 17, a factor 1.13 in the integrated brightness. This was part of a larger dimming from V=0.45 to V=0.84 which occurred between 1994 October and 1995 April (first reported by Guinan and Steelman 1995). We have estimated the photometric variation of Betelgeuse at our ovserving wavelength of 700 nm by comparing the mean flux per frame from our CCD data to that measured for the calibration star (Procyon). The accuracy of this method is limited by the fact that the field of view at the CCD ($2.5''$) was only just larger than the diameter of the seeing disk. However, we find that from November 24 to January 17, the integrated magnitude of Betelgeuse at 700 nm increased by 0.10 ± 0.03, a somewhat smaller change than that of 0.15 magnitudes in the V-band.

4 DISCUSSION

The brightness structure of Betelgeuse continues to show strong asymmetries. The features detected here contribute a similar fraction of the total flux ($\approx 20\%$) to those found in previous interferometric observations (Buscher et al. 1990; Wilson et al. 1992), and their properties remain consistent with a convective origin. For the upper limit hot-spot FWHM of 15 mas, the features would occupy roughly one third of the visible surface area in total. If we assume that the stellar surface and the hot-spots both radiate as blackbodies, then for a mean photospheric temperature of 3500 K, the features would need to have a temperature excess of approximately 600 K in order to provide the 20% contribution seen. This is consistent with the predictions of Schwarzschild (1975) for convection in supergiant stars, although if the features are much smaller than assumed above the implied temperature excess could become embarrassingly large.

In the past, the evolution of surface features has sometimes been suggested as a possible explanation for the irregular variability of Betelgeuse. However our results show that, while the fractional flux contribution from the bright asymmetric features increased slightly from 1994 November to 1995 January, the integrated flux from the star *decreased* significantly over the same period. This is clearly at odds with an explanation for the irregular brightness fluctuations of Betelgeuse in terms of the waxing and waning of surface hot-spots. In this case the spots would be required to fade by at least a factor of two, in order to explain the photometric change, and no such fading was observed. We note that the dimming of Betelgeuse by 0.45 magnitudes from 1994 November to 1995 March was unusually large in comparison to the random V magnitude fluctuations of ± 0.15 typically observed on timescales of a few months (Goldberg 1984), suggesting that different mechanisms may have been involved here.

Although it remains possible that surface hot-spots play a role in the irregular variability of Betelgeuse at other times, we must look elsewhere for an explanation of the sudden dimming at the end of 1994. One alternative scenario is that an episode of mass ejection resulted in dust formation above the star, hence increasing the opacity at visible wavelengths. This has been suggested in the past as an explanation for occasional large, rapid dips in the visual magnitude of Betelgeuse (Goldberg 1984) and is certainly consistent with observations that show the presence of one or more dust shells around the star (Danchi et al. 1994), thereby implying that mass loss is sporadic, with major periods of dust production separated by a few tens of years.

The interferometric data presented here do suggest that a new bright halo has appeared, with a radius $\gtrsim 150$ mas. The properties of this feature are consistent with scattering from a dust shell with a radius approximately five to ten times the photometric radius, i.e. close to the expected dust condensation radius for Betelgeuse (Danchi et al. 1994). Interestingly, recent mid-infrared observations (Bester et al. 1996) have shown evidence for emission from a new structure close to the star, which is interpreted as a dust shell with a radius of approximately $0.1''$. This distance is somewhat smaller than the lower limit for the radius of the large scale optical halo reported here, but is certainly consistent with our measurement given the uncertainties as to the detailed spatial distribution of the dust and its scattering and emission properties.

However, despite this apparent consensus as to the presence of a new dust shell, there is little evidence for an association between the photometric variation of Betelgeuse during our observations with the appearance of new dust. Our NRM results show no significant increase in the fractional flux contribution from the larger scale component between 1994 November and 1995 January. If the visual dimming of 0.15 magnitudes during this time were entirely due to increasing extinction by a thickening (but still optically thin) dust shell, we would have expected the halo to have brightened relative to the disk, since there would also have been more scattering. Furthermore, the flux at mid-infrared wavelengths (around $8-12\,\mu$m), was roughly constant from 1994 November to 1995 January (Bester et al. 1996). The flux at these wavelengths represents only about 1% of the total emission from Betelgeuse, with most of the flux appearing in the visible and near-infrared. If 13% of the optical light (corresponding to the visual dimming from November to January) were absorbed by the dust and re-radiated at longer wavelengths, we would have expected a very large increase in the mid-infrared flux to have occurred.

It is likely, then, that the formation of the new dust halo initially resulted in some fading due to increased absorption, although this took place prior to our first observation in 1994 November. However, the constancy of the "halo" contribution to the total optical flux suggests that the rapid dimming from 1994 November to 1995 January resulted from an intrinsic decrease in the luminosity of the star, presumably due to a change in the temperature and/or diameter of the photosphere. If the change in the V-band magnitude at that time were due to a reduction in the photospheric radius at constant temperature then, for a blackbody emitter, this would imply a reduction of 7%, or approximately 4 mas, in the stellar diameter. Although the uncertainty of the model disk diameters for our NRM data is roughly 2 mas, it is likely that we would have detected a change of this magnitude during the period of our four observations. Furthermore, such an expansion would also have resulted in a 13% reduction in the mid-infrared flux. Alternatively, if the stellar diameter had been fixed, then a reduction in effective temperature from 3500 K to ≈ 3440 K would have produced the 13% dimming observed in the V-band. In this case the 11.15μm flux would also have been reduced, although by a much smaller factor ($\sim 2\%$). Neither of these scenarios match the observations well, but a combination of a 75 K temperature decrease together with a 1% increase in the photospheric radius, would have yielded the observed visual dimming as well as the roughly constant mid-infrared flux. Such a small expansion in diameter (~ 0.5 mas) would not have been detected in the NRM observations.

As well as the overall flux variations, the observed changes in the asymmetric brightness distribution also require explanation. The gradual increase in the asymmetry observed from November 24 to December 24 is well modelled by an increase in the flux contribution from the superposed bright spots, corresponding to a slight brightening of the surface features. The redistribution of flux between 1994 December 24 and 1995 January 17 is somewhat more significant, since there are measurable changes in the azimuthal positions of the spots. Here, a different mechanism may be involved. The long rotation period for Betelgeuse expected on the basis of angular momentum arguments (Smith et al. 1989) appears to rule out rotation as a plausible mechanism for motion of the asymmetries. More likely we have observed convective "boiling", i.e. the turnover of individual turbulent cells at the stellar surface bringing with it hotter material from deeper photospheric layers, and thus a redistribution of the surface intensity pattern.

In closing, it is interesting to compare our visible observations with near-ultraviolet images of Betelgeuse, deconvolved from HST data taken on 1995 March 2-3 (Gilliland & Dupree 1996). Their image at 255 nm shows a very large and heavily limb-darkened disk, with emission extending to at least 125-mas radius. This is interpreted as emission from an extended chromosphere. A single bright unresolved core is also detected, offset by approximately 20 mas from the centre of the intensity distribution. This asymmetry in the UV images is not obviously associated with any of the features in our optical maps. We note however that the UV images were made six weeks after our final observation on January 17. If the UV asymmetry also resulted from convective activity then, in the light of the observations presented here, we might have expected significant changes on this timescale.

The fact that the observation of an extended disk in the UV has coincided with visible and mid-infrared detections of structure around Betelgeuse on similar spatial scales suggests that that the enlargement of the UV disk may also have resulted, at least to some extent, from scattering by dust. In this case a possible alternative explanation for the UV asymmetry is that the dust was distributed asymmetrically about the star. Such an asymmetry would not be entirely unexpected: Schwarzschild (1975) suggested that asymmetries in dust formation might result from large scale convective activity in late type stars, and indeed asymmetries in the dust observed at large distances from Betelgeuse (Bloemhof, Townes & Vanderwyck 1984) suggest that previous episodes of mass loss have been non-isotropic. Coordinated multi-wavelength studies are clearly needed to investigate this possibility.

5 CONCLUSIONS

We have observed a complex bright structure in the surface intensity distribution of Betelgeuse, which changed significantly over a period of eight weeks, and is assumed to result from convective surface activity. However, we find no correlation between the evolution of these features and a rapid dimming of the integrated light from the star during the same period. We have detected a new, circularly symmetric structure around the star with a diameter $\gtrsim 0.3''$, which we interpret as a recently formed dust halo. Since the relative flux contribution from the halo did not increase significantly as the star faded, it appears unlikely that the photometric dimming resulted from increasing absorption by new dust. We conclude that the magnitude increase was due to a global cooling and expansion of the photosphere.

It is clear that further progress in understanding the complex nature of Betelgeuse can be made through the coordination of a range of contemporaneous observations at many wavelengths. For example, coordinated multi-colour photometry and high resolution mapping may yet determine some degree of correlation between the star's irregular variability and changes on the surface. The comparison of imaging observations in the UV (HST) and visible (ground-based interferometry) may allow a determination of the temperature excess of surface features. And the presence of dust and the dynamics of mass loss can perhaps be better understood through simultaneous optical and infrared interferometry, polarimetric observations, and radial velocity measurements.

ACKNOWLEDGEMENTS

The William Herschel Telescope and Carlsberg Automated Meridian Telescope are operated on the island of La Palma by the Royal Greenwich Observatory in the Spanish Observatorio del Roque de los Muchachos of the Instituto de Astrofísica de Canarias. CAH is grateful to the Royal Society for financial support.

REFERENCES

Antia H.M., Citre S.M., Narasimha D., 1984, ApJ, 282, 574
Bedding T.R., Robertson J.G., Marson R.G., 1994, AA, 290, 340
Bester M., Danchi W.C., Hale D., Townes C.H., Degiacomi C.G., Mekarnia C.G., Geballe T.R., 1996, ApJ, 463, 336
Bloemhof, E.E., Townes, C.H., Vanderwyck, A.H.B., 1984, ApJL, 276, L21.
Buscher D.F., Haniff C.A., Baldwin J.E., Warner P.J., 1990, MNRAS, 245, 7p
Danchi W.C., Bester M., Degiacomi C.G., Greenhill L.J., Townes C.H., 1994, AJ, 107, 1469
Gilliland R.L., Dupree A.K., 1996, ApJL, 463, L29
Guinan, E., Steelman D., 1995, IAU Circ. 6150.
Goldberg L., 1984, PASP, 96, 366
Haniff C.A., Mackay C.D., Titterington D.J., Sivia D., Baldwin J.E., Warner P.J., 1987, Nature, 328, 694
Hayes D.P., 1981, PASP., 93, 752
Krisciunas K., Luedeke K.D., 1996, Information Bulletin on Variable Stars, no. 4355. Konkoly Obs, Budapest (Hungary), 2p
Pearson T.J., Readhead A.C.S., 1984, Ann Rev Astron Astrophys, 22, 97
Schwarz H.E., Clarke D., 1984, AA, 132, 370
Schwarzschild M., 1975, ApJ, 195, 137
Sivia D.S., 1987. *PhD thesis*, Cambridge University.
Smith M.A., Patten B.M., Goldberg L., 1989, AJ, 98, 2233
Tinbergen J., Greenberg J.M., de Jager C., 1981, AA, 95, 215
Tuthill P.G., Haniff C.A., Baldwin J.E., 1997, MNRAS, in press.
Wilson R. W., Baldwin J.E., Buscher D.F., Warner P.J., 1992, MNRAS, 257, 369